Name of participant: Chenchang Jiang

School: Shenzhen College of International Education

Province: Guangdong

Country/Region: China

Advisor1: Erjun Chen

Affiliation of the advisor: Qingshen Senior High School

Advisor2: Yiting Su

Affiliation of the advisor: Shenzhen College of International

Education

Title: Rapid Screening of TCRm Antibody Based on Micro-well

Array for Cancer Immunotherapy

#### Rapid Screening of TCRm Antibody Based on Micro-well Array for

#### **Cancer Immunotherapy**

# Chenchang Jiang Shenzhen College of International Education

#### **Abstract**

The discovery of T-cell receptor mimic (TCRm) antibodies remains a bottleneck in translational immunotherapy due to the low efficiency and long timelines of conventional hybridoma and phage display platforms. Here, we present a rapid single-cell screening approach using an agarose micro-well array capable of capturing ~3.5×10<sup>5</sup> cells per chip. This platform achieved ~90% single-cell occupancy and identified  $\sim\!2\%$  of wells as antigen-specific antibody secreting cells, corresponding to an estimated ~6.3×10<sup>3</sup> candidate clones per screening. Compared to limiting dilution cloning, which yields only ~10-30% efficiency and requires weeks of sequential subcloning, our system enabled primary fluorescence-based readout within 3-4 hours and downstream validation via flow cytometry and confocal imaging within days. By eliminating antigen pre-coating and reducing reagent consumption, this pipeline shortens the antibody discovery timeline while maintaining functional validation within a single experimental workflow. This advantage is particularly applicable for TCRm antibodies, which target intracellular antigens presented on MHC and are notoriously rare and difficult to isolate compared to conventional monoclonal antibodies. Although validation was limited to in vitro assays, these proof-of-concept results demonstrate a scalable and cost-effective improvement to traditional methods, with the potential to accelerate preclinical development of therapeutic TCRm antibodies.

**Keywords:** T-cell receptor mimic antibody, immunotherapy, microwell array, antibody screening

# Contents

Abstract2
1. Introduction5
2. Methods&materials
2.1. Cell and reagents
2.2. The preparation of microwell array7
2.3. The preparation of single-cells array8
2.4. The detection of secreting antibody8
2.5. The screening of secreting antigen-specific antibody
2.6. Flow cytometry
2.7. Confocal fluorescent microscope9
3. Results
3.1. The characterization of microwell array10
3.2. The characterization of single-cell array
3.3. Successful detection of secreting antibody11
3.4. Rapid screening of secreting antigen-specific antibody12
3.5. The verification of antibodies using Flow cytometry
3.6. The specific binding of antibodies to tumor cells using
fluorescence imaging
3.7. Comparative performance with limiting dilution
4. Discussion

References	20
Acknowledgement	22
	A No
	CO-XIV
	CONTIN
5 -1/	<b>X</b>
70.7	
00,14,	
V	

#### 1. Introduction

Cancer remains one of the leading causes of mortality worldwide, accounting for approximately one in every six deaths<sup>1</sup>. Conventional treatment modalities—including surgery, chemotherapy, and radiation therapy—form the backbone of clinical oncology but exhibit significant limitations. Surgical resection often fails to remove microscopic disease completely, necessitating combination therapies, while chemotherapy and radiotherapy are hindered by systemic toxicity and the risk of recurrence due to tumour heterogeneity<sup>2</sup>.

In contrast, immunotherapy represents a paradigm shift by leveraging the patient's own immune system to selectively target cancer cells. Among immunotherapies, immune checkpoint inhibitors, targeting programmed cell death-1/programmed cell death-1 ligand (PD-1/PD-L1) and cytotoxic T lymphocyte antigen-4 (CTLA-4), have demonstrated remarkable clinical efficacy in otherwise refractory cancers, including metastatic melanoma and non-small-cell lung cancer<sup>3-5</sup>. Yet, despite these advances, immune checkpoint blockade alone benefits only a subset of patients. As a result, combination strategies are actively being pursued to enhance responsiveness and durability of therapeutic benefit<sup>6,7</sup>.

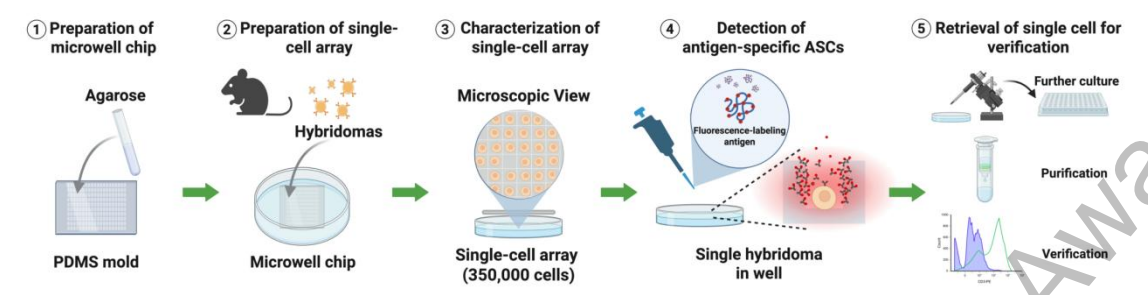
Beyond checkpoint inhibition, therapeutic monoclonal antibodies (mAbs) have become indispensable in oncology, serving as tumour-targeting agents, antibody-drug conjugates (ADCs), and bispecific T-cell engagers (BiTEs)<sup>8-10</sup>. These antibodies, developed primarily through hybridoma technology and phage display platforms, have enabled the development of highly specific biologics with improved therapeutic indices<sup>11-13</sup>. Hybridoma-based techniques allow for in vivo affinity maturation and full-length immunoglobulin G (IgG) production, whereas phage display permits high-throughput screening and the generation of fully human antibodies with reduced immunogenicity<sup>8, 14</sup>.

However, a key challenge persists: conventional antibody discovery pipelines are costly, time-intensive, and involve complex engineering steps, such as enzyme-linked immunosorbent assay (ELISA) for hybridoma cell screening, and antibody

humanization in phage display<sup>15, 16</sup>. Accelerating early-phase antibody screening while reducing costs is therefore a critical unmet need in cancer immunotherapy. Recent advances in microfabrication and biomaterials have opened the door for cost-effective antibody screening platforms<sup>17, 18</sup>. Traditional methods for antibody validation and hybridoma cell line screening require limited dilution, which is time consuming, inefficient, and probabilistically disadvantaged<sup>19</sup>. Recently developed methods often require coating microarrays with antigen-specific antibodies or recombinant antigens—a process that is laborious, expensive, and not easily scalable, and therefore highly limiting in terms of throughput<sup>20, 21</sup>.

In contrast, agarose-based micro-well arrays offer a versatile and economical alternative<sup>22</sup>. Agarose is biocompatible, easy to process, and potentially provides structural integrity for trapping single cells in defined wells, allowing for greater scalability and eliminating the need for antibody pre-coating while reducing material waste<sup>23</sup>.

Building on this principle, we successfully developed a single-cell micro-well chip composed of agarose and polydimethylsiloxane (PDMS) molds, enabling high-throughput screening of T-cell receptor mimic (TCRm) antibodies at the single-cell level. Unlike conventional antigen-coated arrays, this approach captures hybridoma or cancer cells directly in micro-wells, streamlining subsequent antibody-antigen interaction assays. Our system provides rapid and high-resolution insights into antibody specificity and binding efficacy. This platform demonstrates a scalable, cost-effective, and high-throughput alternative to conventional antibody screening pipelines. By minimizing reagent consumption, eliminating antigen pre-coating steps, and providing real-time single-cell resolution, our approach has the potential to accelerate preclinical antibody discovery for immuno-oncology applications. Future improvements could incorporate automated cell-loading, integrated imaging analytics, and microfluidic enhancements, paving the way for industrial-scale screening platforms and personalized immunotherapy development.



Scheme 1. Schematic illustration of the workflow of rapid screening of TCRm antibody based on micro-well array. Step 1 Preparation of the microwell chip: Agarose is cast into a PDMS mold to form a microwell array suitable for single-cell isolation. Step 2 Preparation of the single-cell array: Hybridoma cells are seeded into the microwell chip to achieve single-cell distribution. Step 3 Characterization of the single-cell array: Microscopic observation confirms the formation of a single-cell array containing approximately 350,000 individual cells. Step 4 Detection of antigen-specific antibody-secreting cells (ASCs): Fluorescence-labeled antigen is applied to identify hybridomas secreting antigen-specific antibodies. Step 5 Retrieval of single cells for verification: Selected hybridomas are retrieved for further culture, antibody purification, and binding verification via flow cytometry and confocal microscopy.

#### 2. Methods&materials

#### 2.1. Cell and reagents

Hybridomas were cultured in RPMI 1640 culture medium supplemented with 10% fetal bovine serum (FBS) and 1% penicillin/streptomycin (P/S) (complete culture medium). KMS26 and AU565 cells were cultured in DMEM culture medium with 10% FBS and 1% P/S. All cells were cultured under 37 °C with 5% CO<sub>2</sub>.

## 2.2. The preparation of microwell array

A 1% (w/v) agarose solution was prepared by dissolving 1 g of agarose powder in 100 mL of distilled water. The solution was heated in a microwave oven to ensure complete dissolution, then cooled to approximately 80 °C for 20 minutes. A total of 800 μL of the agarose solution was pipetted onto a polydimethylsiloxane (PDMS) mold, followed immediately by the placement of a pre-cleaned glass coverslip to form a thin, uniform gel layer. After cooling at room temperature for 10 minutes, the agarose solidified into a structured micro-well array with high cohesion and defined micro-wells. Coverslips were

washed with distilled water, and PDMS molds were cleaned by gentle tapping to remove dust and residual agarose. The PDMS mold was then placed in a standard 6-cm diameter cell culture dish and immersed in 1% PBS buffer solution under UV light., stored in a biosafety cabinet.

#### 2.3. The preparation of single-cells array

Frozen hybridoma cells were thawed in a 37.0 °C water bath and vortexed until homogeneous. The suspension was centrifuged at 1000 rpm for 4 minutes, and the supernatant was discarded. The pellet was resuspended in RPMI1640 complete culture medium. A 500 μL aliquot of the hybridoma suspension was gently applied to the agarose micro-well array surface dropwise and incubated for 15 minutes in 37.0 °C with 5% CO<sub>2</sub> to allow cells to settle into individual wells. Excess liquid was carefully removed by pipetting. Two rounds of phosphate-buffered saline (PBS) washing (1000 μL each) were performed to remove untrapped or loosely attached cells. Microscopic images of the resulting single-cell arrays were captured using a digital camera attached to a light microscope. All experiments were independently repeated three times using separate microwell chips to ensure reproducibility. Negative controls included antigen-negative cell lines and isotype antibody controls where appropriate.

#### 2.4. The detection of secreting antibody

If cell trapping was unsuccessful, the preparation of single-cell array was repeated. Fluorescent secondary antibodies Anti-Mouse IgG Fab2 Alexa Fluor (R) 594 Molecular probes were then added to the single-cell microarray chip in a 1:200 ratio relative to saturated culture media. Successful binding was then screened and observed as rings of red fluorescence around individual wells under infrared light and photographed via light microscope.

# 2.5. The screening of secreting antigen-specific antibody

The antigens were labelled with Alexa Fluor 647 (red) fluorescence using Alexa Fluor Succinimidyl Esters (Thermofisher scientific) following the manufacturer's instructions. The labeled pHLA was added into RPMI-1640 medium at a final concentration of 10 µg/mL in a

6-cm plate containing a single cell microwell chip loaded with hybridomas. The hybridomas were cultured for 3 hours in a CO<sub>2</sub> incubator. Following incubation, the single cell microwell chip were scanned and imaged using fluorescence microscope. The red fluorescence ring around a single hybridoma indicated antigen-specific antibody binding. In contract, the absence of an fluorescence ring surrounding a single hybridoma was considered no antibody or non-specific antibody secretion. Using the single cell obtaining device, fluorescence rings surrounding hybridomas on the single cell microwell chip were analyzed; selected single hybridomas were automatically isolated and transferred into individual wells of a 96-well plate for further clonal expansion and antibody production. Across three independent runs, the retrieval success rate of selected clones averaged ~70%, with the majority of recovered cells remaining viable for subsequent expansion.

#### 2.6. Flow cytometry

Samples consisting of 30  $\mu$ L of KMS26 and AU565 cancer cell lines were prepared in Eppendorf tubes. For each type of TCRm antibody under investigation, 1  $\mu$ L was pipetted into its designated micro-well, aligned with corresponding single cells on the array. After a 30-minute incubation, fluorescently labeled secondary antibodies (1  $\mu$ L, diluted in 100  $\mu$ L of ddH<sub>2</sub>O) were added to each well, followed by an additional 30-minute incubation. The array was centrifuged at 1200 rpm for 3 minutes to remove unbound antibodies. Supernatant was discarded and replaced with 300  $\mu$ L of PBS. Following washing, samples were imaged under a light microscope to visualize fluorescent signals indicating successful antibody binding.

#### 2.7. Confocal fluorescent microscope

To validate the binding specificity of the TCRm antibodies, samples were further processed for confocal fluorescence microscopy. Cell suspensions were centrifuged and diluted to a final volume of 2.4 mL with PBS. Then, 10 μL of each TCRm antibody (10 antibodies) was added into separate cell samples (KMS26 or AU565), respectively. Fluorescent secondary antibodies used for detection included Fab<sub>2</sub> Alexa Fluor® 594-labeled anti-mouse IgG (Molecular Probes), prepared at a 1:200 dilution in saturated culture medium. Fluorescence imaging was performed to assess the localization and intensity of antibody

binding at the single-cell level, providing a rapid and visual means of screening candidate TCRm antibodies.

#### 3. Results

#### 3.1. The characterization of microwell array

To evaluate the physical integrity and structure of the agarose-PDMS micro-well array, we fabricated chips using 1% agarose and imaged them under bright-field microscopy. As shown in Figure 1a, the micro-wells exhibited uniformity in size and consistent spacing, with scale bars indicating 120 to 500 µm, suitable for capturing single cells. These observations confirm that the agarose-based array successfully meets the geometric requirements for single-cell screening, demonstrating feasibility for subsequent functional assays.

# 3.2. The characterization of single-cell array

To verify the efficiency of single-cell occupation, hybridoma suspensions were deposited on the microwell arrays and observed microscopically following washing. Figure 1b displays examples of occupied and unoccupied wells, demonstrating that cells could be isolated reliably in individual chambers without overlap or aggregation. The successful formation of single-cell arrays is critical for downstream functional analysis, confirming the system's compatibility with compartmentalized screening protocols. Figure 1c represents quantitative analysis of single-cell occupancy rate, with approximately  $\sim 90\%$  occupation rate across n=6 randomly selected fields. This reflects the high success rate of cell occupation in our method, coinciding with our goals of achieving high-throughput in antibody screening. Notably, the observed occupancy rate ( $\sim 90\%$ ) significantly exceeded the theoretical single-cell occupancy predicted under limiting dilution at  $\mu \approx 0.3$  ( $\sim 22\%$ , p < 0.01, Chi-square test), underscoring the efficiency of the microwell approach.

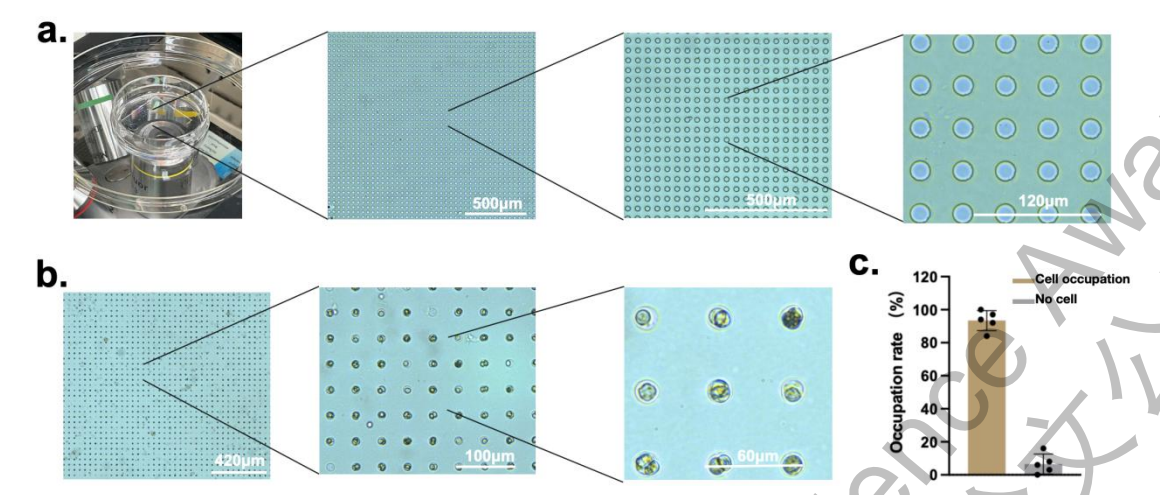


Figure 1. The characterization of microwell chip and single-cell array. (a) Image of the prepared agarose microwell array cast in a 3.5-cm Petri dish, shown under low magnification, with progressively magnified views highlighting the uniform arrangement and consistent dimensions of the microwells (scale bars:  $500 \, \mu m$ ,  $500 \, \mu m$ ,  $120 \, \mu m$ ). (b) Representative bright-field images following hybridoma cell seeding, demonstrating uniform distribution of individual cells within microwells (scale bars:  $420 \, \mu m$ ,  $100 \, \mu m$ ,  $60 \, \mu m$ ). (c) Quantitative analysis of single-cell occupancy rate, showing a high proportion of wells containing single cells (mean  $\pm$  SD, n = 6 randomly selected fields, across n = 3 technical replicates).

#### 3.3. Successful detection of secreting antibody

To detect general antibody secretion, Alexa Fluor 594-conjugated secondary antibodies were added to the hybridoma-loaded microwell arrays. As illustrated in Figure 2a, and magnified specific examples in Figure 2b, hybridomas secreted varying levels of IgG antibodies, visualized by red fluorescent rings encircling the wells. Varying degrees of secretion were compared in complementary couples in Figure 2b: strong secretion, cell present (1); no secretion, cell present (2); weak secretion, cell absent (3); and weak secretion, cell escaped (4). Figures 2c displays a quantitative analysis of the varying degrees of secretion across n = 6 randomly selected fields. Approximately  $\sim 96\%$  of cells showed no secretion, with approximately 2% and 1% showing weak and strong secretion respectively. The measure of high discrimination (1% measure of strong secretion) reflects a high degree of specificity, coinciding with our goals of screening for high-specificity antibodies. This fluorescence-based classification demonstrates that the microarray platform effectively distinguishes hybridoma clones based on secretion intensity at the single-cell level.

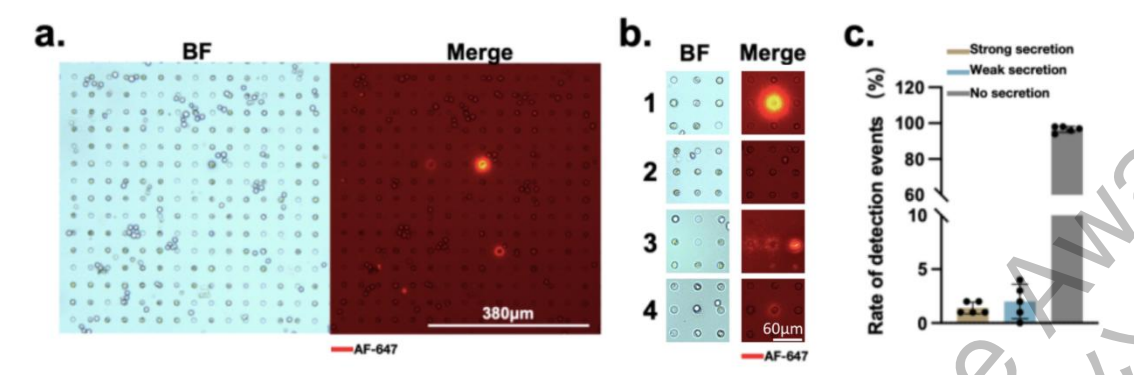


Figure 2. The successful detection of secreting antibody using fluorescence-labeling antibody. (a) Representative bright-field (BF) and merged fluorescence images showing single hybridoma cells seeded in microwells, with secreted antibodies detected via AF-647-labeled antigen binding (red signal). Wells containing secreting cells display localized fluorescence halos surrounding the cell. Scale bar: 380  $\mu$ m. (b) Higher magnification BF and merged images illustrating examples of strong secretion, cell present (1); no secretion, cell present (2); weak secretion, cell absent (3); and weak secretion, cell escaped (4). Scale bar: 60  $\mu$ m. (c) Quantification of detection rates for strong, weak, and non-secreting hybridoma cells (n = 6 random fields; error bars = SD; across n = 3 technical replicates).

# 3.4. Rapid screening of secreting antigen-specific antibody

To evaluate antigen specificity, AF647-labeled peptide-MHC complexes were added to hybridoma-containing arrays, followed by imaging under fluorescence microscopy. In Figure 3a, red fluorescence rings indicated specific antigen binding, while wells without such rings represented either non-secreting or non-specific antibody-secreting cells. Figure 3b represented a magnification of cells 1 and 2 selected as examples in Figure 3a, illustrating the difference between secreting cells and non-secreting/non-specific cells. Figure 3c represents quantitative analysis of occupation rate of antigen-specific cells. With an occupation rate of approximately 2% across 6 randomly selected fields, the high specificty of antibody secreting cell lines detected further support our goal of screening for highly specific antibodies. The system reliably distinguished specific binders from background, validating its capacity for functional TCRm antibody screening without the need for antigen immobilization.

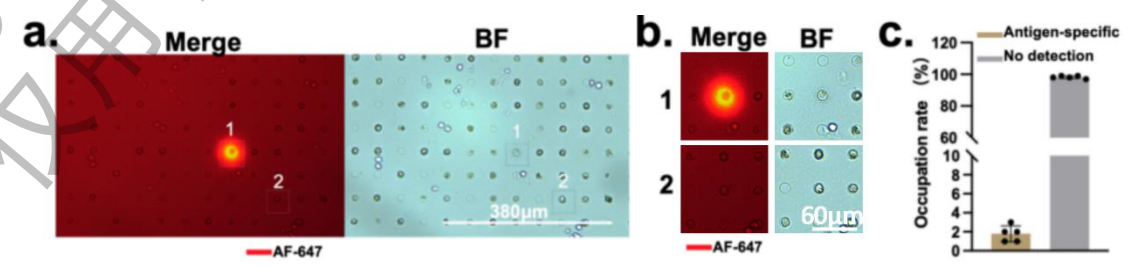
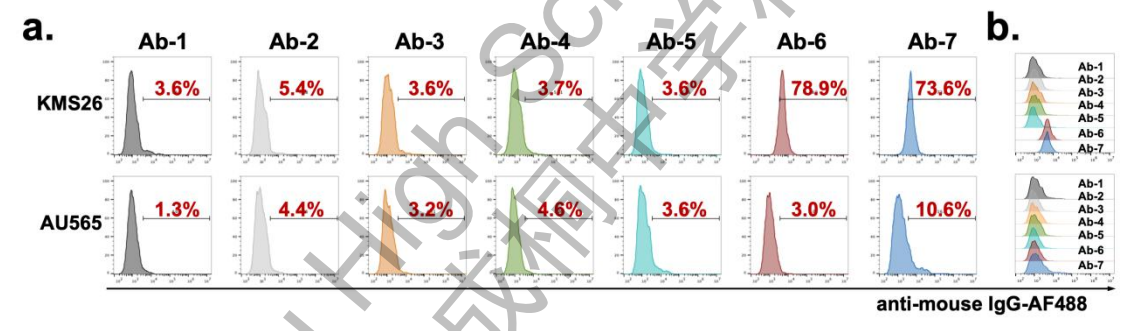


Figure 3. The successful detection of secreting antibody using fluorescence-labeling antigen. (a) Merged AF-647 fluorescence and bright-field (BF) images of microwells containing single hybridomas, with antigen-specific secretion indicated by strong AF-647 signals (well 1) compared to absence of signal (well 2). (b) Enlarged views of wells 1 and 2 confirm antigen-specific secretion in well 1 and no detectable secretion in well 2. (c) Quantification of detection results showing the proportion of antigen-specific ASCs versus wells with no detection (mean  $\pm$  SD, n = 6 random fields per chip, across n = 3 technical replicates).

### 3.5. The verification of antibodies using Flow cytometry

To quantitatively assess specificity of TCRm antibody candidates, flow cytometry was conducted using KMS26 and AU565 cancer cell lines. As shown in Figure 4a-4b, a panel of antibodies (Ab-1 to Ab-7) exhibited variable binding ability, with Ab-3 (5.4%) and Ab-4 (4.4%) displaying higher positivity compared to others (1.3%-3.7%). These results indicate that the screening platform can effectively triage TCRm clones based on antigen recognition capability, providing a scalable and semi-quantitative readout.



**Figure 4. Purified antibody verified using flow cytometry.** (a) Representative histograms showing binding of purified antibodies (Ab-1 to Ab-7) to target cell lines KMS26 and AU565 (representative histograms from one of n = 3 technical replicates). Percentage values (in red) indicate the proportion of cells positively stained with anti-mouse IgG-AF488 for each antibody. (b) Overlay plots of all seven antibodies for each cell line, illustrating differences in binding profiles. High binding is observed for Ab-6 and Ab-7 against KMS26, and for Ab-7 against AU565, indicating antigen specificity, while other antibodies display low or negligible binding.

# 3.6. The specific binding of antibodies to tumor cells using fluorescence imaging

To further validate antigen-specific binding at the cellular level, KMS26 and AU565 cells were incubated with selected antibodies and analyzed by confocal microscopy. KMS26 is a tumor cell line known to express the target antigen, whereas AU565 lacks this target and serves as a negative control. Based on the flow cytometry results (Figure 4a-4b), Ab-6 and

Ab-7 exhibited the strongest binding activity among all candidates, and were therefore selected for additional imaging experiments.

As shown in Figure 5a-5b, clear AF488 fluorescence was observed on the surface of KMS26 cells treated with Ab-6 and Ab-7, while AU565 cells displayed negligible signals. The green AF488 signal was predominantly localized at the cell membrane, consistent with antigen-specific binding, while DAPI staining confirmed nuclear localization. Together, these results confirm that antibodies identified through the micro-well screening platform not only bind effectively to their intended antigen but also retain this specificity in intact cancer cells.

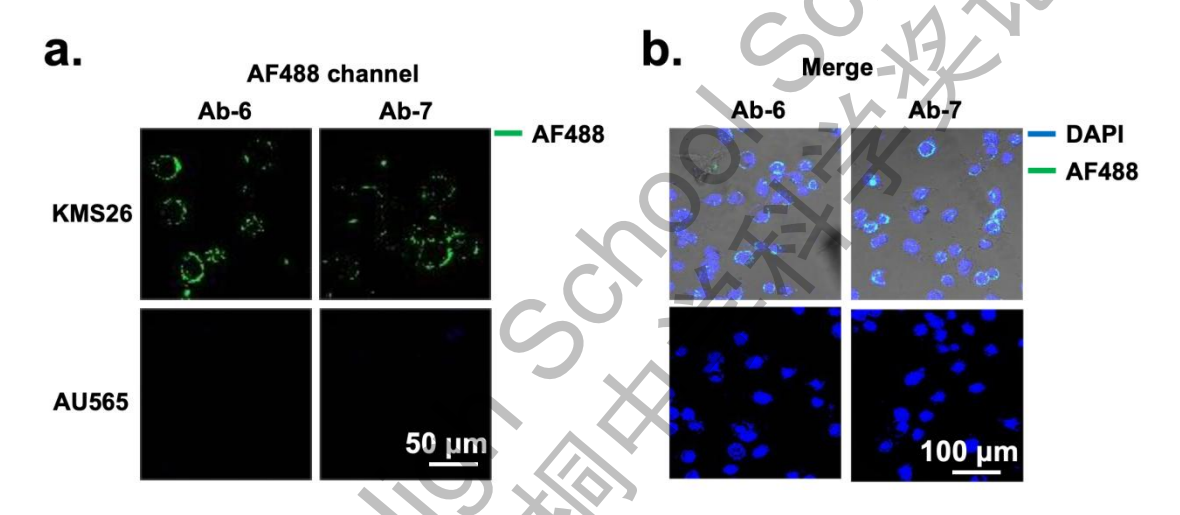


Figure 5. Verification of purified antibodies using confocal fluorescence microscopy. Representative confocal images showing binding of purified antibodies Ab-6 and Ab-7 to KMS26 cells (top row) and lack of detectable binding to AU565 cells (bottom row) (representative confocal images from one of n = 3 technical replicates). (a) AF488 channel images show antibody binding visualized with Alexa Fluor 488 (green). (b) Merged images with DAPI-stained nuclei (blue) highlight the cellular localization of antibody binding. Scale bars: 50  $\mu$ m (a) and 100  $\mu$ m (b).

# 3.7. Comparative performance with limiting dilution

To contextualize the performance of our agarose microwell array, we compared its statistical outcomes to traditional limiting dilution cloning. The Poisson distribution governing limiting dilution predicts that, at  $\mu\approx0.3$  cells/well, only ~22% of wells will contain exactly one cell while ~74% remain empty, necessitating multiple rounds of recloning and yielding reported single-cell cloning efficiencies of only ~10-30%<sup>24</sup>. By contrast, our platform achieved ~90% single-cell occupancy (Fig. 1c), with ~2% of wells showing antigen-specific

secretion (Fig. 3c). Extrapolated to the ~3.5×10<sup>5</sup> microwells per chip, this corresponds to ~6.3×10<sup>3</sup> candidate wells identified in a single screen. Detection occurred within hours via fluorescence (Figs. 2-3) and was confirmed by flow cytometry and confocal imaging (Figs. 4-5), compressing a workflow that ordinarily requires weeks into a single experimental cycle. This compression of screening into a single cycle, with hours-scale primary readout (Figs. 2-3) and downstream confirmation (Figs. 4-5), highlights the microwell array's superior throughput and sensitivity. A side-by-side statistical summary is presented in Table 1.

Metric	Limiting dilution (hybridoma)	Agarose microwell array (this study)	Linked Figures
Throughput per run	~10 <sup>2</sup> –10 <sup>3</sup> wells (96–384 plates)	~3.5×10 <sup>s</sup> wells per chip	Scheme 1; Fig. 1a
Single-cell occupancy	Poisson at μ≈0.3 → ~22% single-cell, ~74% empty	~90% single-cell occupancy	Fig. 1c
Antigen-specific "hit" rate	Typically requires multiple ELISA rounds; low	~2% of occupied wells antigen-specific	Fig. 3c
Time to readout	Days-weeks (growth + ELISA, recloning)	Hours (fluorescence) to days (flow/confocal)	Figs. 2–5
Rounds to monoclonality	≥2-3	1 (chip enforces single-cell)	Fig. 1b–c
Expected antigen-specific clones/run	Highly variable; often low	$\sim 6.3 \times 10^3 = (3.5 \times 10^5 \times 0.9 \times 0.02)$	Fig. 1c; Fig. 3c
Reagent use / cost	High (antigen coating, ELISA reagents, subcloning)	Lower (no pre-coating; localized diffusion)	Methods, Fig. 2a–c

Table 1. Comparative statistics between limiting dilution and microwell array screening. Values for limiting dilution cloning efficiency ( $\sim$ 10-30%) are from de St Groth & Scheidegger (1980)<sup>24</sup>. All microwell array metrics (throughput, occupancy, antigen-specific detection rate) are derived from this study (Figs. 1-3). "Expected antigen-specific clones/run" was estimated as total wells ( $3.5\times10^5$ ) × mean occupancy ( $\sim$ 0.9) × antigen-specific frequency ( $\sim$ 0.02). Time to readout and reagent use are approximate and reflect standard workflows (ELISA and recloning for limiting dilution vs fluorescence/flow cytometry for microwell arrays). Abbreviations: ELISA, enzyme-linked immunosorbent assay.

#### 4. Discussion

The present study establishes a proof-of-concept for an agarose micro-well array platform designed to overcome the inefficiencies of conventional antibody discovery. By integrating single-cell isolation with fluorescence-based secretion assays, flow cytometry, and confocal imaging, we achieved a complete pipeline from screening to validation within days rather than weeks. Our platform demonstrated  $\sim 90\%$  single-cell occupancy and  $\sim 2\%$  antigen-specific detection (Figs. 1–3), translating into  $\sim 6.3 \times 10^3$  candidate clones per chip. In contrast, limiting dilution cloning is statistically constrained by Poisson distribution, typically yielding only  $\sim 10-30\%$  efficiency and requiring multiple rounds of recloning<sup>24</sup>. These comparative results (Table 1) highlight the superior throughput, speed, and sensitivity of the microwell approach.

A critical advantage of the agarose micro-well array is its ability to preserve local microenvironments around individual cells. In conventional limiting dilution or bulk assays, secreted antibodies rapidly diffuse into the culture medium, lowering local concentrations and raising the risk of false negatives. In the microwell format, antibodies remain compartmentalized, creating localized zones of high concentration around secreting cells. This greatly enhances detection sensitivity and allows discrimination between strong, weak, and non-secreting clones (Fig. 2). Such compartmentalization also reduces the risk of cross-contamination between clones, a recurring challenge in supernatant-based ELISAs. These design features explain, at least in part, the superior resolution and specificity we observed relative to traditional approaches.

Another critical consideration is the minimization of false positives and negatives. In traditional supernatant-based ELISAs, antibody diffusion can cause false positives through cross-well contamination, while dilutional effects contribute to false negatives by lowering local antibody concentration below detection thresholds. By maintaining secretion products within confined microwells, our platform reduces both risks, ensuring more accurate identification of true antigen-specific clones.

The comparison with limiting dilution provides one benchmark, but it is equally important to consider alternative discovery platforms. Phage display, for example, offers

high-throughput screening but requires recombinant antigen preparation, antibody engineering, and often downstream humanization. Similarly, antigen-coated microarrays necessitate costly antigen immobilization and may fail to capture conformational epitopes relevant to native tumor environments. In contrast, our agarose-based system requires no pre-coating, reduces reagent consumption, and interrogates antibodies secreted under physiologically relevant conditions. These distinctions position the microwell array as a complementary tool that bridges the gap between the scalability of phage display and the functional relevance of hybridoma-derived antibodies.

Our findings further suggest that direct antigen labeling (Fig. 3) provides more reliable readouts than secondary antibody labeling (Fig. 2). Antigen labeling yielded clear fluorescence halos around positive clones, whereas antibody-labeled assays occasionally produced ambiguous signals. This difference underscores the importance of assay design in minimizing background and improving specificity. Flow cytometry (Fig. 4) and confocal imaging (Fig. 5) subsequently confirmed that candidates identified through antigen labeling retained specificity against target cell lines, validating the robustness of the screening pipeline. Statistical reasoning further reinforces the advantage of this approach. Under limiting dilution at  $\mu$ <0.3, the probability of exactly one cell per well is only ~22%, with ~74% of wells empty and the remainder often containing multiple cells. Our observed ~90% single-cell occupancy (Fig. 1c) represents a significant improvement over this theoretical baseline, effectively compressing weeks of subcloning into a single experimental cycle. Moreover, by increasing the number of wells per run (~3.5×10<sup>5</sup> vs ~10<sup>3</sup> in plate-based systems), the effective sampling size increases by two orders of magnitude, lowering the risk of missing rare, high-affinity clones.

Despite these advantages, several limitations remain. The number of validated antibodies was modest, reflecting both the restricted input pool and potential losses during loading and retrieval. Our validation relied primarily on in vitro assays, leaving open questions regarding stability, pharmacokinetics, and tumor-targeting efficiency in vivo. In addition, the platform was tested against a narrow antigen panel. Expanding this to a broader range of tumor-associated antigens will be essential to assess the generalizability of the approach. Technical limitations also exist: agarose chips can be fragile during handling, and the current

workflow still requires manual microscopy. Integrating microfluidic delivery, automated imaging, and AI-based image analysis could further improve reproducibility and throughput.

Clinically, the implications are significant. TCRm antibodies are an emerging class with the potential to target intracellular antigens presented on MHC, thereby expanding the therapeutic landscape beyond traditional cell-surface markers. However, their discovery is hindered by low yields and stringent specificity requirements. A platform that can rapidly recover rare, high-specificity clones in a single cycle could shorten preclinical development timelines from weeks to days, reduce costs, and enable more personalized antibody generation. This is especially critical for TCRm antibodies, which recognize intracellular peptide–MHC complexes and therefore expand the therapeutic landscape to targets inaccessible to conventional surface-binding antibodies. Their rarity and specificity requirements make rapid, high-throughput recovery methods particularly valuable. In resource-limited settings, the reduction in antigen and reagent requirements could also democratize access to advanced antibody discovery methods.

Future work should build on these strengths. Scaling the system to larger input pools will allow for the recovery of even rarer clones. Incorporating orthogonal assays such as ELISA, Western blotting, or surface plasmon resonance (SPR) would provide complementary binding data and kinetic information. Integration with AI-driven image analysis and high-content screening platforms could further enhance throughput by enabling automated recognition of fluorescence patterns and reducing human bias in interpretation.. Most importantly, preclinical testing in animal models will be critical to confirm therapeutic potential, biodistribution, and off-target effects. In parallel, collaboration with industrial partners could help translate this proof-of-concept into a robust pipeline for antibody discovery at scale.

In summary, this study demonstrates that agarose micro-well arrays represent a powerful alternative to traditional antibody discovery platforms. By achieving ~90% occupancy, ~2% antigen-specific detection, and thousands of candidate clones per run, this system offers unmatched throughput and sensitivity relative to limiting dilution. While limitations remain, the integration of compartmentalized single-cell screening with functional validation provides a blueprint for accelerating TCRm antibody discovery. With further optimization and translational validation, this platform could play a transformative role in developing

next-generation immunotherapies.

#### References

- 1. The global challenge of cancer. *Nat Cancer* **2020**, *1* (1), 1-2.
- 2. Zafar, A.; Khatoon, S.; Khan, M. J.; Abu, J.; Naeem, A., Advancements and limitations in traditional anti-cancer therapies: a comprehensive review of surgery, chemotherapy, radiation therapy, and hormonal therapy. *Discov Oncol* **2025**, *16* (1), 607.
- 3. Rowshanravan, B.; Halliday, N.; Sansom, D. M., CTLA-4: a moving target in immunotherapy. *Blood* **2018**, *131* (1), 58-67.
- 4. Zhang, H.; Liu, L.; Liu, J.; Dang, P.; Hu, S.; Yuan, W.; Sun, Z.; Liu, Y.; Wang, C., Roles of tumor-associated macrophages in anti-PD-1/PD-L1 immunotherapy for solid cancers. *Mol Cancer* **2023**, *22* (1), 58.
- 5. Lee, D.; Cho, M.; Kim, E.; Seo, Y.; Cha, J. H., PD-L1: From cancer immunotherapy to therapeutic implications in multiple disorders. *Mol Ther* **2024**, *32* (12), 4235-4255.
- 6. Saha, M.; Chakraborty, C.; Arun, I.; Ahmed, R.; Chatterjee, S., An Advanced Deep Learning Approach for Ki-67 Stained Hotspot Detection and Proliferation Rate Scoring for Prognostic Evaluation of Breast Cancer. *Sci Rep* **2017**, *7* (1), 3213.
- 7. Arrieta, V. A.; Dmello, C.; McGrail, D. J.; Brat, D. J.; Lee-Chang, C.; Heimberger, A. B.; Chand, D.; Stupp, R.; Sonabend, A. M., Immune checkpoint blockade in glioblastoma: from tumor heterogeneity to personalized treatment. *J Clin Invest* **2023**, *133* (2), e163447.
- 8. Nelson, A. L.; Dhimolea, E.; Reichert, J. M., Development trends for human monoclonal antibody therapeutics. *Nat Rev Drug Discov* **2010**, *9* (10), 767-774.
- 9. Colombo, R.; Tarantino, P.; Rich, J. R.; LoRusso, P. M.; de Vries, E. G. E., The Journey of Antibody-Drug Conjugates: Lessons Learned from 40 Years of Development. *Cancer Discov* **2024**, *14* (11), 2089-2108.
- 10. Huehls, A. M.; Coupet, T. A.; Sentman, C. L., Bispecific T-cell engagers for cancer immunotherapy. *Immunol Cell Biol* **2015**, *93* (3), 290-296.
- 11. Zhang, C., Hybridoma technology for the generation of monoclonal antibodies. *Methods Mol Biol* **2012**, *901*, 117-135.
- 12. Jaroszewicz, W.; Morcinek-Orłowska, J.; Pierzynowska, K.; Gaffke, L.; Węgrzyn, G., Phage display and other peptide display technologies. *FEMS Microbiol Rev* **2022**, *46* (2), fuab502.
- 13. Alfaleh, M. A.; Alsaab, H. O.; Mahmoud, A. B.; Alkayyal, A. A.; Jones, M. L.; Mahler, S. M.; Hashem, A. M., Phage Display Derived Monoclonal Antibodies: From Bench to Bedside. *Front Immunol* **2020**, *11*, 1986.
- 14. Li, W.; Yang, W.; Liu, X.; Zhou, W.; Wang, S.; Wang, Z.; Zhao, Y.; Feng, N.; Wang,
- T.; Wu, M.; Ge, L.; Xia, X.; Yan, F., Fully human monoclonal antibodies against Ebola virus possess complete protection in a hamster model. *Emerg Microbes Infect* **2024**, *13* (1), 2392651.
- 15. Stanker, L. H.; Hnasko, R. M., A Double-Sandwich ELISA for Identification of Monoclonal Antibodies Suitable for Sandwich Immunoassays. *Methods Mol Biol* **2015**, *1318*, 69-78.
- 16. Rossotti, M. A.; Bélanger, K.; Henry, K. A.; Tanha, J., Immunogenicity and humanization of single-domain antibodies. *Febs j* **2022**, *289* (14), 4304-4327.
- 17. Gharib, G.; Bütün, İ.; Muganlı, Z.; Kozalak, G.; Namlı, İ.; Sarraf, S. S.; Ahmadi, V. E.; Toyran, E.; van Wijnen, A. J.; Koşar, A., Biomedical Applications of Microfluidic Devices: A Review. *Biosensors (Basel)* **2022**, *12* (11), 1023.
- 18. Lyle, D. B.; Bushar, G. S.; Langone, J. J., Screening biomaterials for functional complement

- activation in serum. J Biomed Mater Res A 2010, 92 (1), 205-13.
- 19. Greenfield, E. A., Single-Cell Cloning of Hybridoma Cells by Limiting Dilution. *Cold Spring Harb Protoc* **2019**, Nov 1, *2019* (11).
- 20. Jin, H.; Zangar, R. C., Antibody microarrays for high-throughput, multianalyte analysis. *Cancer Biomark* **2010**, *6* (5-6), 281-290.
- 21. Rho, J. H.; Lampe, P. D., High-throughput screening for native autoantigen-autoantibody complexes using antibody microarrays. *J Proteome Res* **2013**, *12* (5), 2311-2320.
- 22. Goodarzi, S.; Lux, F.; Rivière, C., Evaluating Nanoparticles Penetration by a New Microfluidic Hydrogel-Based Approach. *Methods Mol Biol* **2024**, *2804*, 223-235.
- 23. Khodadadi Yazdi, M.; Taghizadeh, A.; Taghizadeh, M.; Stadler, F. J.; Farokhi, M.; Mottaghitalab, F.; Zarrintaj, P.; Ramsey, J. D.; Seidi, F.; Saeb, M. R.; Mozafari, M., Agarose-based biomaterials for advanced drug delivery. *J Control Release* **2020**, *326*, 523-543.
- 24. de StGroth, S. F.; Scheidegger, D., Production of monoclonal antibodies: strategy and tactics. *J Immunol Methods* **1980**, *35* (1-2), 1-21.

#### Acknowledgement

In presenting the agarose microwell array project, I extend my deepest gratitude to all those who have provided support, guidance, and encouragement throughout this research. First and foremost, I take the opportunity to acknowledge my teachers, Mr. Chen and Ms. Su, who served as my primary supervisors. Their guidance was entirely voluntary and unpaid; a reflection of their dedication to nurturing students' academic growth. They were instrumental in providing direction at key stages of the project. Mr. Chen guided me through experimental design and analysis, ensuring that my methods were rigorous and feasible within the available resources. Ms. Su offered valuable insights during the data interpretation and paper-writing stages, helping me refine my scientific arguments and improve the clarity of my writing. Their mentorship was not only academic but also inspirational, cultivating in me a greater passion for biology and scientific research.

The topic of this project, developing a platform for rapid screening of TCRm antibodies using an agarose-based microwell array, arose from my own interest in immunotherapy and its potential to revolutionize cancer treatment. After reviewing recent literature and identifying the critical bottleneck in the current screening modus, I proposed the idea to my supervisors, who encouraged me to explore its feasibility. Together, we discussed the limitations of traditional antibody discovery methods and the advantages of adapting single-cell microarray technology, laying the foundation for the experimental plan.

I was responsible for conducting the literature review, preparing the experimental design, fabricating the agarose microwell chips, performing cell culture, and carrying out fluorescence and flow cytometry experiments. I also completed the data collection, analysis, and visualization of results. My supervisors provided oversight during laboratory experiments to ensure safety and accuracy, and they reviewed my data interpretation to confirm scientific soundness. In writing this paper, I drafted the manuscript, while my supervisors gave constructive feedback to help me revise and polish the final paper.

Several challenges arose during the project. Initially, fabricating microwell arrays of consistent size and depth proved difficult, which led to uneven single-cell distribution. To overcome this, I adjusted the agarose concentration and optimized the molding technique

under the guidance of my teachers. Another difficulty occurred during antibody detection: background fluorescence interfered with signal clarity. Through repeated trials and consultation, I was able to refine the staining protocol, reducing noise and improving reproducibility. These problem-solving experiences were invaluable, as they strengthened both my technical skills and resilience as a researcher.

I am also grateful to the University of Science and Technology of China and the Shenzhen College of International Education for providing access to essential experimental equipment, including flow cytometers and confocal microscopes. Without these resources, it would have been impossible to complete the project to its current level. I also extend my gratitude to all the scientists whose work is cited herein; their pioneering research provided the theoretical and methodological foundation upon which my project is built.

I extend special appreciation towards my former biology teacher, Dr. Gasanoff, who offered general advice on academic writing. His suggestions greatly improved the structure and readability of the manuscript, ensuring that my ideas were communicated more effectively.

I also thank my peers, who provided feedback during the writing process, and my family, who supported me emotionally throughout the project. Their encouragement allowed me to stay focused and motivated even in moments of doubt.

In conclusion, this project was the result of collaborative effort and support from many individuals and institutions. While the experiments and manuscript were primarily my independent work, the guidance of my teachers, the provision of resources from my school and research institutions, and the encouragement from family and peers were indispensable. I am deeply grateful to all who have contributed to this journey.